Green Chemistry

Accepted Manuscript

ROYAL SOCIETY OF CHEMISTRY

www.rsc.org/greenchem

Green Chemistry

ARTICLE

Predictive screening of ionic liquids for dissolving cellulose and experimental verification

Received 00th January 20xx,
Accepted 00th January 20xx

DOI: 10.1039/x0xx00000x

www.rsc.org/

Yan-Rong Liu,[a,b,c] Kaj Thomsen,[b] Yi Nie,[c] Suo-Jiang Zhang,*[c] Anne S. Meyer*[a]

In this work, 357 ionic liquids (ILs) formed from 17 cations and 21 anions were selected for evaluation of their ability to dissolve cellulose by COSMO-RS. In order to evaluate the predictive model and method, experimental measurements of the solubility of microcrystalline cellulose (MCC) in 7 of these ILs were also conducted. Predicted results from logarithmic activity coefficients were generally in good agreement with the experimental results. Three different models were used for describing cellulose, and the mid-monomer part of the cellotriose model was found to be closer to the experimental results than a neat glucose model and the model of the mid-dimer part of cellotetraose. Excess enthalpy calculations indicated that hydrogen-bond (H-bond) interactions between cellulose (i.e. the three cellulose models) and the 7 studied ILs are key factors for the solubility of cellulose, and the anions play a crucial role in the cellulose dissolution process. Importantly, the cations of methylimidazolium$^+$, pyridinium$^+$, ethylmorpholinium$^+$ and methylpyrrolidinium$^+$ structured with functional groups including ethyl, allyl, 2-hydroxylethyl, 2-methoxyethyl and acryloyloxypropyl, combined with anions Ac^-, Dec^-, $HCOO^-$, Cl^-, BEN^-, $DMPO_4^-$, DEP^-, DBP^- and Br^- were predicted to be the best for dissolving cellulose.

1. Introduction

Cellulose is widely used in paper products, textiles, plastics, coatings, composites, laminates, optical film, pharmaceuticals and other applications. The numerous applications of cellulose is attributed to its promising features, such as biocompatibility, biodegradability, thermal and chemical stability.[1,2] Cellulose is a linear polymer consisting of several hundred to over ten thousand β-(1→4)-linked glucose repeating units, together with numerous intermolecular and intramolecular H-bonds.[3,4] The multiple H-bonds between cellulose molecules form highly ordered crystalline regions which makes cellulose insoluble in water and common organic solvents.[5] Some traditional solvent systems have been investigated for cellulose dissolution processes, for example, N-methylmorpholine oxide (NMMO),[6] N, N-dimethylacetamide/lithium chloride (DMAc/LiCl),[7] N, N-dimethylformamide/nitrous tetroxide (DMF/N_2O_4),[8] molten salt hydrates ($LiClO_4{\cdot}3H_2O$, $LiCH_3COO{\cdot}2H_2O$, $LiCl/ZnCl_2/H_2O$, $NaSCN/KSCN/LiSCN{\cdot}2H_2O$),[9,10] and aqueous NaOH or aqueous solutions of metal complexes (Cd-tren, Ni-tren and Cuoxam).[11] However, drawbacks of these processes including high cost, high dissolution temperature, volatility, difficulty in solvent recovery and toxicity make them undesirable, and underlines the necessity for developing greener solvents for cellulose dissolution.[12,13] Ionic liquids (ILs) can be considered green solvents[14-17]. In the recent years, more than 60 ILs have been investigated for their ability to dissolve cellulose.[3] The increasing interest in ILs as solvents is due to their remarkable properties such as immeasurably low vapour pressure, excellent chemical and thermal stability, electrical conductivity, and non-flammability. The most fascinating property of ILs is the structural diversity, as numerous possible cations and anions can be combined freely.[3,18,19]

It is reported that the best cations for dissolving cellulose are mainly derivatives of imidazolium and pyridinium,[3] and that the most efficient anions are chloride, acetate, formate, phosphate, sulphate, and sulfonate.[20] Some researchers claim that the cellulose dissolution process is strongly anion-dependent,[3,21,22] whereas others claim that not only the properties of anions or cations, but also their combination, make ILs efficient for dissolving cellulose.[23] Erdmenger[24] and Zhao[25] indicated that cations can influence the dissolution of cellulose. Increasing the alkyl chain length of the cation decreases the ability of the IL to dissolve cellulose. By adjusting the functional groups on the cations of ILs, more efficient and functionalized ILs for dissolving cellulose can be obtained. Li et al.[26] concluded that AmimCl with a double bond is more effective in dissolving cellulose than BmimCl. Luo et al.[27] synthesized 1-(2-hydroxyethyl)-3-methyl imidazolium chloride (HOEtmimCl) and found that ILs containing hydroxyl groups on the imidazole cation are excellent solvents for dissolving cellulose due to the H-bonds formation with cellulose. The

---

[a] *Center for Bioprocess Engineering, Department of Chemical and Biochemical Engineering, Technical University of Denmark, Søltofts Plads 227, 2800, Lyngby, Denmark, E-mail: am@kt.dtu.dk.*

[b] *Center for Energy Resources Engineering (CERE), Department of Chemical and Biochemical Engineering, Technical University of Denmark, Søltofts Plads 229, 2800, Lyngby, Denmark, E-mail: kth@kt.dtu.dk.*

[c] *Beijing Key Laboratory of Ionic Liquids Clean Process, Key Laboratory of Green Process and Engineering, State Key Laboratory of Multiphase Complex Systems, Institute of Process Engineering, Chinese Academy of Sciences, P.O. Box 353, Beijing, 100190, China, E-mail: sjzhang@ipe.ac.cn.*

†Electronic Supplementary Information (ESI) available: General synthesis processes and the properties of the ILs studied in this work. See DOI: 10.1039/x0xx00000x

solubility of microcrystalline cellulose (MCC) in HOEtmimCl can reach 5%-7% at 70 °C. However, cellulose has a low solubility in [H(OEt)$_3$mim]Ac because the flexibility of [H(OEt)$_3$mim]Ac allows it to form H-bonds with its anions, which decreases the cellulose solubility.[28]

Numerous possible ILs composed of cations and anions can be synthesized. The functional groups of the cations can be modified to affect the capacity of ILs to dissolve cellulose. It is nevertheless a challenge to identify the best ILs for dissolving cellulose. A rapid and a priori screening method to predict the cellulose solubility capacity for ILs is needed in chemical engineering research and industry. COSMO-RS (Conductor-like Screening Model for Real Solvents), integrates dominant interactions of H-bonds, misfits, and Van der Waals forces in IL systems to summarize multiple solvation.[29] COSMO-RS can be used for performing mixture calculations at various temperatures, which renders it considered by many to be the most accurate model for the prediction and development of ILs for specific tasks currently available.[30]

Previous publications have demonstrated that COSMO-RS can successfully predict properties of ILs in the field of biomass dissolution, such as activity coefficients,[31] solubilities[32-34] and excess enthalpies[35]. Activity coefficient calculations have been shown to be useful for predicting cellulose solubility in ILs.[36] Kahlen et al.[37] found that the anion played an important role in dissolving cellulose according to COSMO-RS calculations. Casas et al.[22] studied the solubility of cellulose and lignin in different ILs using activity coefficient and excess enthalpy calculations from COSMO-RS. They reported activity coefficients and excess enthalpies with similar tendencies, and demonstrated that the exothermal behaviour and low activity coefficients of cellulose and lignin in ILs was related to higher solubilities. [22] On the basis of that work, Casas et al.[35] subsequently designed 3 × 3 cellulose model structures consisting of nine “differently cut” monomers, M1 to M9, to be used by COSMO-RS to represent cellulose. Based on the calculated activity coefficients, excess enthalpies and the experimental results for 12 ILs, the M4 model was finally selected as the best cellulose model.[35]

The aims of this work were to use COSMO-RS to screen potential ILs for their ability to dissolve cellulose and to select the best cellulose model from three cellulose models considered. These three cellulose models investigated included a glucose model (Model 1), a mid-monomer part of a cellotriose model (Model 2), and a mid-dimer part of a cellotetraose model (Model 3). The ILs tested in this work mainly focused on 17 cations based on methylimidazolium$^+$, pyridinium$^+$, ethylmorpholinium$^+$ and methylpyrrolidinium$^+$ structures with ethyl, allyl, 2-hydroxyethyl, 2-methoxyethyl and acryloyloxypropyl functional groups. The 17 cations were combined with 21 different anions. The solubility of MCC in seven different ILs was measured experimentally to verify the predictions of the logarithmic activity coefficients and excess enthalpies of the three cellulose models in the ILs. The best cellulose model was then identified by comparing the predictions with the experimental results.

2. Computational details and calculation sets of cellulose models and ionic liquids

2.1 COSMO-RS computation details

The COSMO-RS calculations were carried out using several procedures. First, the quantum chemical Gaussian09 package was used to optimize the structure of the studied compounds at the B3LYP/6-31++G (d, p) level. Second, the COSMO files of the optimized structures were opened by Gaussian03 and COSMO continuum solution models were calculated using the BVP86/TZVP/DGA1 level theory. Third, the logarithmic activity coefficients, excess enthalpies, σ-potentials and σ-profiles were determined using the model COSMO-RS (implementation: COSMOtherm version C3.0 release 14.01, applied with parameterization BP_TZVP_C30_1401, COSMOlogic, Leverkusen, Germany). The calculation temperature for COSMO-RS was set to 90 °C, the same temperature as used for the experimental determination of cellulose solubility.

When conducting calculations in the COSMO-RS program, the molar fractions of the cations and anions of the ILs were treated as equal, i.e. $n_{cation}=n_{anion}=n_{IL}$.[35] The logarithmic activity coefficients and excess enthalpies for solutions of cellulose in ILs were also investigated by COSMO-RS. In these two calculations, the molar fraction of cellulose was set as 0.5, the molar fraction of the IL cations was set as 0.25, and the molar fraction of the IL anions was set as 0.25. The activity coefficients and the excess enthalpies were calculated according to the COSMO-RS theory. The activity coefficient calculation equation has been described previously by Diedenhofen and Klamt,[31] and the excess enthalpy equation has been described by Gonzalez-Miquel et al..[38]

2.2 Cellulose models

The program package COSMOtherm has several methods to model a polymer. Usually, only one or several repeating units are selected for the calculation. Then, the end group of the polymer is deactivated using a function of COSMO-RS called “weight string”, which allows for selectively switching on/off certain atoms within a COSMOfile. [36] Using this function, with the weight string code for off being “0” and for on being “1”, the weight string sequences for each atom in the mid-monomer part of a cellotriose model and the mid-dimer part of a cellotetraose model were obtained (Fig. 1). For this configuration, the total free energy of each model was calculated as the sum of its DFT/COSMO energy in the conductor reference state and its individual pseudo chemical potential, obtained from the COSMO-RS model.[37] In this case, three representations were selected for cellulose, and these structures were obtained according to the procedures described in section 2.1-2.2. The resulting chemical structures and charge surface regions are displayed in Fig. 1.

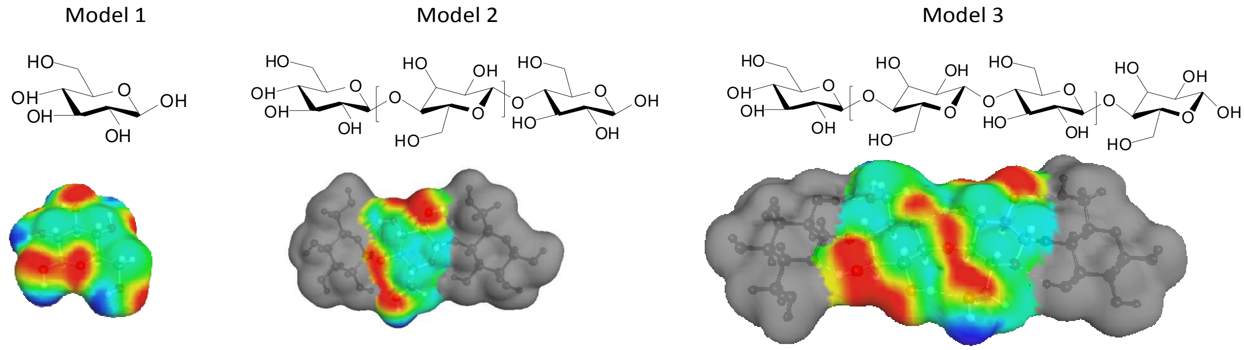

w= {000000000000000000000000111111111111111111111
11111111110000000000000000000000}

w= {00000000000000000000001111111111111111111111
1111111111111111111100000000000000000000000000}

Fig. 1 COSMO-RS charge surfaces of three cellulose representation models: Model 1: Glucose; Model 2: Mid-monomer of cellotriose; Model 3: Mid-dimer of cellotetraose. Red zones indicate a positive surface charge, yellow and green zones indicate almost neutral charges, navy blue designate negative surface charge. The code-sequences inside the brackets correspond to the weight string codes for each model: "0" indicates that the atom was deactivated (switched "off") and "1" indicates that the atom was activated (switched "on") in the COSMO-RS calculation.

2.3 Structure of cations and anions

The structure of cations and anions employed in this work can be seen in Table 1 and Table 2 respectively. The COSMOfiles for the cations No. 1-5, 10-13, and 14-17 in Table 1 and all the COSMOfiles for the anions in Table 2 come from the COSMO-RS database. The COSMOfiles for the cations No. 6-9 in Table 1 were calculated based on the procedures outlined in 2.1.

According to the work of Wang et al.[3] imidazolium-based and pyridinium-based ILs which have the functional groups alkyl-, allyl-, hydroxyl-, ether- and ester- are potential for dissolving cellulose. Morpholinium-based and pyrrolidinium-based ILs with these function groups were considered based on the works of Raut et al.[39] and Zavrel et al..[40] The cations of methylimidazolium$^+$, pyridinium$^+$, ethylmorpholinium$^+$ and methylpyrrolidinium$^+$ with functional groups of ethyl, allyl, 2-hydroxylethyl, 2-methoxyethyl or acryloyloxypropyl were combined with 21 anions resulting in the 357 ILs studied in this work.

Table 1 Cations studied in this work

No.	Name of cation	Acronym	Structure
1-5	1-R-3-methylimidazolium	[Emim, Amim, HOEtmim, EtOMmim, AOPmim] R=ethyl, allyl, 2-hydroxylethyl, 2-methoxyethyl, acryloyloxypropyl	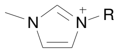
6-9	N-R-pyridinium	[Epy, Apy, HOEtpy, EtOMpy] R=ethyl, allyl, 2-hydroxylethyl, 2-methoxyethyl	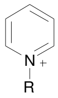
10-13	4-R-4-ethylmorpholinium	[Eemor, Aemor, HOEtemor, EtOMemor] R=ethyl, allyl, 2-hydroxylethyl, 2-methoxyethyl	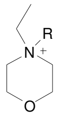
14-17	1-R-1-methylpyrrolidinium	[Empyrr, Ampyrr, HOEtmpyrr, EtOMmpyrr] R=ethyl, allyl, 2-hydroxylethyl, 2-methoxyethyl	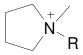

Table 2 Anions studied in this work

No.	Name of anion	Acronym	Structure	No.	Name of anion	Acronym	Structure
1	Acetate	Ac	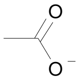	12	Formate	HCOO	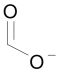
2	Tetrachloroaluminate	$AlCl_4$	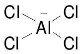	13	Hydrogensulfate	HSO_4	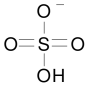
3	Bromide	Br	Br^-	14	Iodide	I	I^-
4	Tetrafluoroborate	BF_4	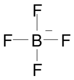	15	Methoxyethylsulfate	$MeOEtSO_4$	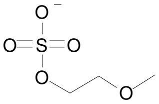
5	Butylsulfate	$BuSO_4$	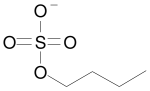	16	Methylsulfate	$MeSO_4$	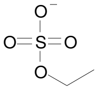
6	Benzoate	BEN	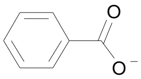	17	Dicyanamide	$N(CN)_2$	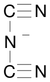
7	Chloride	Cl	Cl^-	18	Hexafluorophosphate	PF_6	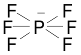
8	Perchlorate	ClO_4	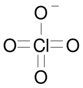	19	Bis(trifluoromethylsul -fonyl)amide	Tf_2N	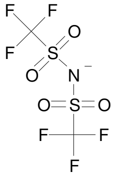
9	Dimethylphosphate	$DMPO_4$	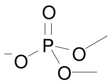	20	Toluene-4-sulfonate	Tos	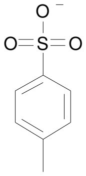
10	Diethylphosphate	DEP	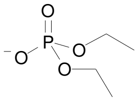	21	Decanoate	Dec	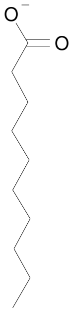
11	Dibutylphosphate	DBP	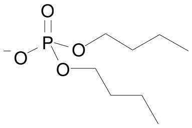				

Green Chemistry

ARTICLE

3. Results and discussion

3.1 σ-potential of three cellulose models

In COSMO-RS, σ-potential is a measure of the affinity of the system to a surface of polarity σ. The σ-potential can be divided into three main regions: the H-bond donor region ($\sigma < -0.0082$ e/Å^2), the H-bond acceptor region ($\sigma > +0.0082$ e/Å^2), and the non-polar region ($-0.0082 < \sigma < +0.0082$ e/Å^2).[38] Fig. 2 shows that the σ-potential values of Model 1 are more negative than those of Model 2 and Model 3 in the H-bond acceptor region, which means that Model 1 gives more affinity for H-bond acceptor surfaces than the other two models.

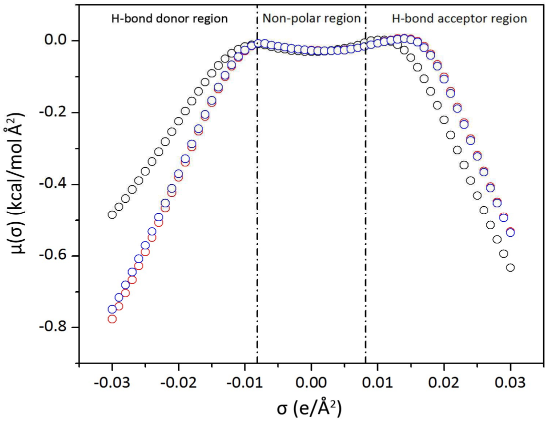

Fig. 2 σ-potentials of Model 1 (black circle), Model 2 (blue circle) and Model 3 (red circle) predicted by COSMO-RS

3.2 Logarithmic activity coefficient prediction by COSMO-RS

The predicted logarithmic activity coefficients (lnγ) of the three cellulose models in each of the 357 ILs are depicted in Fig. 3–Fig. 5. The cations and anions are listed according to their cellulose dissolution ability. The ILs with high cellulose dissolution capacities according to the predicted logarithmic activity coefficients are located to the left, while the ILs with lower cellulose dissolution capacities are located to the right. The logarithmic activity coefficients of these three cellulose models in different ILs varied significantly with the use of different anions (Fig. 3 – Fig. 5), suggesting that the cellulose dissolution capacity is mostly determined by the anion while the cation only has a moderate effect on the dissolution process. In particular, the methylpyrrolidinium-based ILs have a remarkably high predicted logarithmic activity coefficient, which may be due to its ability to form H-bonds with cellulose. The anions Ac$^-$, Dec$^-$, HCOO$^-$, Cl$^-$, DEP, DMPO$_4$$^-$, DBP$^-$, BEN$^-$ and Br$^-$ were predicted to be best anions for dissolving cellulose. Our results are in agreement with the findings of Kahlen et al.[37] and Casas et al.[22] Kahlen et al.[37] gave an explanation for this phenomenon: The energy of the H-bonds of cellulose is up to 25 kJ/mol,[41] thus the interactions between cellulose and solvent need to go beyond this energy in order to result in cellulose dissolution. This requires that either the cation or the anion of the IL is highly polar and the combination of the anion and cation is only slightly polar. Tabulated values of the predicted logarithmic activity coefficients for cellulose in ILs can be found in the supporting information.

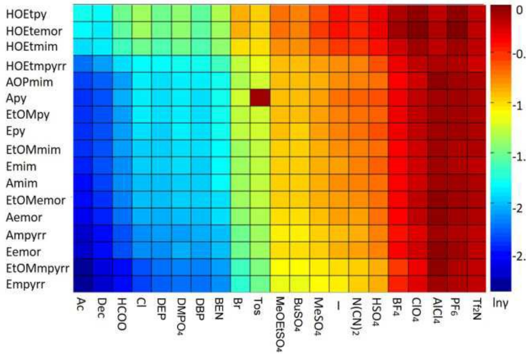

Fig. 3 The logarithmic activity coefficients prediction of model 1 in 357 ILs. Conditions: the mole fraction of cellulose model 1 was 0.5, the mole fraction of IL cations and anions was 0.25 each. The calculation temperature was 90 °C.

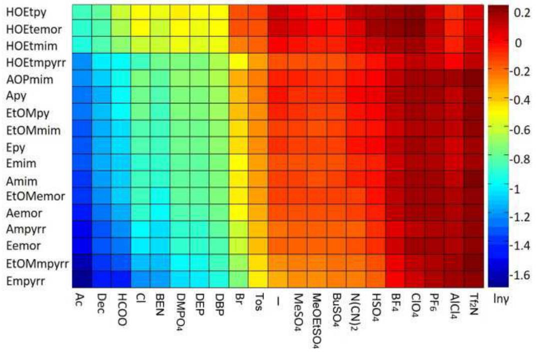

Fig. 4 The logarithmic activity coefficients prediction of model 2 in 357 ILs. Conditions: the mole fraction of cellulose model 2 was 0.5, the mole fraction of IL cations and anions was 0.25 each. The calculation temperature was 90 °C.

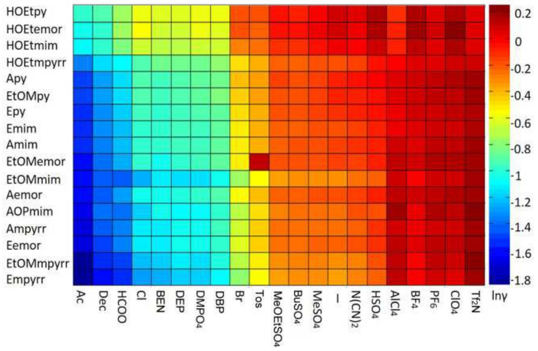

Fig. 5 The logarithmic activity coefficients prediction of model 3 in 357 ILs. Conditions: the mole fraction of cellulose model 3 was 0.5, the mole fraction of IL cations and anion was 0.25 each. The calculation temperature was 90 °C.

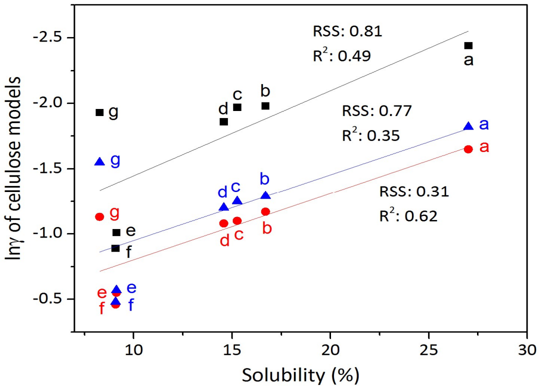

Fig. 6 Experimental values of MCC solubilities in seven ILs plotted against lnγ: Model 1 (■), Model 2 (●) and Model 3 (▲).

Table 3 Experimental solubility of MCC in seven ILs and COSMO-RS prediction results for the three cellulose models

No.	ILs	Solubility (wt%)	Solubility (g/mol IL)	ln γ prediction results by COSMO-RS		
				Model 1	Model 2	Model 3
a	EmimAc	27	46	-2.44	-1.65	-1.82
b	AmimCl	＜17	＜26	-1.98	-1.17	-1.29
c	EmimDEP	15	40	-1.97	-1.10	-1.25
d	ApyCl	15	23	-1.86	-1.08	-1.20
e	HOEtmimBr	9.1	19	-1.01	-0.55	-0.57
f	HOEtpyBr	9.1	18	-0.89	-0.46	-0.48
g	EtOMmimCl	8.3	15	-1.93	-1.13	-1.55

3.3 Experimental solubility in seven ILs

In Fig. 3 – Fig. 5, the ILs are sorted according to their ability to dissolve cellulose. The best IL for cellulose dissolution appears in the lower left corner of each of the three charts. It should be noted that the cations appear in almost the same order in Fig. 3 and Fig. 4. In Fig. 5, the order of the cations is slightly different. However, the order of the anions is almost identical in each of the figures. In order to validate the COSMO-RS prediction results and obtain the best model to represent cellulose, the solubility of cellulose in seven ILs was measured at 90 °C. These seven ILs were chosen mainly because they contain the functional groups ethyl, allyl, 2-hydroxylethyl, or 2-methoxyethyl with methylimidazolium$^+$ and pyridinium$^+$ as the cations (section 2.3). Ac$^-$, Cl$^-$, DEP$^-$, Br$^-$ were selected as the anions because the prediction of logarithmic activity coefficients showed that these anions are efficient for cellulose dissolution (Fig. 3-5). EmimAc has previously been identified as having superior properties for cellulose dissolution.[35] In addition, three types of comparisons for cellulose dissolution capacity can be distinguished among the seven ILs chosen: 1. EmimAc and EmimDEP have the same imidazolium cation but different anions, 2. AmimCl and EtOMmimCl have the same anion but different imidazolium cations, and 3. The sets of AmimCl/ApyCl and HOEtmimBr/HOEtpyBr have the same anions but different kinds of cations (one is an imidazolium cation, the other is a pyridinium cation). Table 3 shows that except for [EtOMmim]Cl, the ILs have dissolution trends identical to the logarithmic activity coefficient trends. Predictive quantitative modelling by COSMO-RS calculations can thus be used to qualitatively assess and notably rank the ability of different ILs to dissolve cellulose. Casas et al.[35] (using a selected monomeric structure (M4) inside a 3×3 cellulose macrostructure as cellulose model) and Kahlen et al.[37] (using the mid-monomer glucose unit of cellotriose as a cellulose model) have previously predicted the abilities of different ILs to dissolve cellulose, but some of their predictions turned out not to be consistent with the experimental results. Kahlen et al.[37] explained the reason for divergence between prediction and experimental results as being due to that water might be hindering the interaction between IL and cellulose.

In this work, HOEtmimBr and HOEtpyBr turned out to have a higher water content than the rest of ILs (shown in the ESI), which might explain the deviation between the predicted and the experimental result (point e, f being off the linear correlation in Fig. 6). Casas et al.[35] studied the cellulose dissolving property of EtOEmimCl which contains the ether functional group by predicting the activity coefficient in COSMO-RS. Casas et al.[35] reported the activity coefficient (γ) of EtOEmimCl to be 0.61 and that of HOEtmimBr to be 1.32 meaning that EtOEmimCl was predicted to have a better cellulose dissolving capacity than HOEtmimBr (as they concluded cellulose to be soluble when $\gamma < 0.85$ in their selected model for cellulose). In the present work we also consistently found that the predicted logarithmic activity coefficient, $\ln\gamma$, of EtOMmimCl was lower than that of HOEtmimBr (Table 3), which was in agreement with the prediction tendency of Casas et al..[35] However, the experimental result slightly contrasted the prediction result between EtOMmimCl and HOEtmimBr, and showed that EtOMmimCl fitted poorly to the fitting line (Table 3 and Fig. 6), but it needs to be added that both solvents had low cellulose dissolution capacity with < 10 wt% cellulose solubility.

Kahlen et al.[37] reported contradictions between predictions and experimental results for BmimCl and BmimAc. The prediction result from COSMO-RS documented that BmimAc had a better cellulose dissolving capacity than BmimCl, but, according to the experimental result reported by Vitz et al.[42] the cellulose solubility of BmimCl is 20%, and that of BmimAc is 12%. Kahlen et al.[37] explained that the ability of Chloride to form hydrogen bonds is not yet totally clear and difficult to model properly in COSMO-RS, which may explain why experimental results and prediction data for ILs with Chloride anion do not always agree. Fig. 6 indicates that the residual sum of squares (RSS) of Model 2 is smaller and R square (R^2) is larger than the other two models. Hence, the prediction results of Model 2 were best correlated with the experimental solubility results. According to the predicted logarithmic activity coefficients of these three models, the logarithmic activity coefficients of Model 1 were significantly lower than the logarithmic activity coefficients of the other two cellulose models. This might be explained by the Model 1 being too simple to represent cellulose.[35]

3.4 Excess enthalpy prediction by COSMO-RS

The excess enthalpies from the intermolecular interactions (H-bonds, misfits and Van der Waals forces) between the cellulose models and seven ILs were calculated by COSMO-RS (Fig. 7). The histogram in Fig. 7 illustrates that the H-bond interactions between the three cellulose models and the cations and anions of ILs have a high influence on the solubility of cellulose in the IL, followed by misfit and Van der Waals force interactions. ILs with the same cations and different anions, such as EmimAc and EmimDEP, exhibit excess enthalpies that are very different. However, when the ILs have the same anion and different cations, the excess enthalpies have similar values. This is valid for the two bromides and the chloride in Fig. 7 (Model 1 and Model 2), which indicates that the anions play a crucial role in the dissolution process. These two results are in agreement with the study of Casas et al.[35] Casas et al.[22] indicated that H-bond energy values predicted by COSMO-RS reflects the affinity of ILs and cellulose, that is higher energy values of H-bonds qualitatively reflect higher solubility of cellulose in ILs. The molecular dynamics simulation works of Huo et al.[43] elucidated that the anions interact much more strongly with the cellulose surface than the cations. In their paper, they show that the main driving force for the cellulose dissolution is the H-bonds formed between anions of ILs and hydroxyl groups of cellulose, and this is supported here by the excess enthalpy result. It is observably in Fig. 7 that the excess enthalpy of EtOMmimCl in Model 3 is more negative than the excess enthalpy of EmimDEP and AmimCl. This is in disagreement with the experimentally determined solubility of cellulose in EtOMmimCl, thus Model 3 is not a good model to represent cellulose.

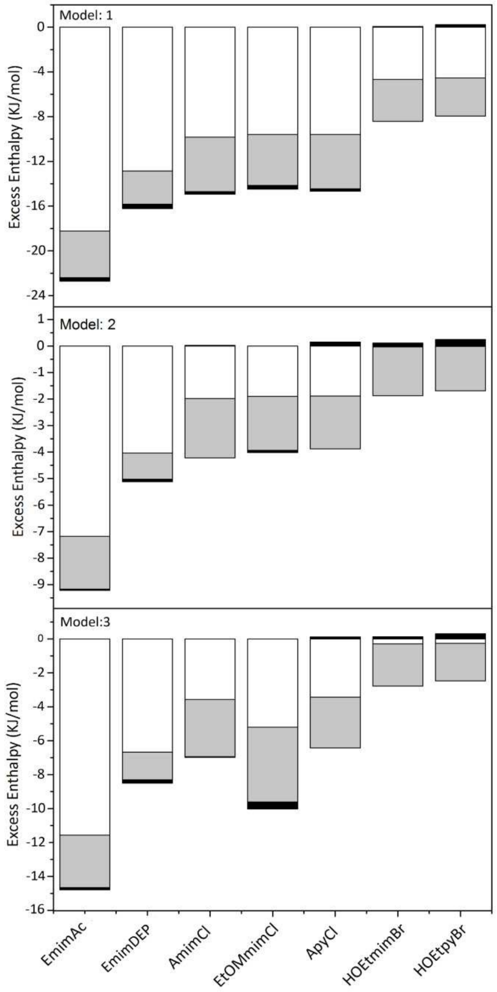

Fig. 7 Excess enthalpies between the three cellulose models and seven ILs, H-bond (white histogram), misfit (grey histogram) and Van der Waals force (black histogram)

3.5 σ-profiles prediction by COSMO-RS

The logarithmic activity coefficient and excess enthalpy prediction results illustrated that the cellulose dissolution process is strongly anion-dependent. Additionally, the σ-profiles between three cellulose models and the anions of Ac^{-}, DEP^{-} and BEN^{-} shown in Fig. 8 further describe the possible interactions of the three models and the anions. The σ-profiles of the candidates show that Ac^{-} and the three cellulose models are almost complementary, while DEP^{-} is not as complementary result within the nonpolar region. This means that with the same cations, Ac^{-} the presence of the Ac^{-} renders the IL a better cellulose solvent than DEP^{-}. This is in agreement with the experimental results, which showed that EmimAc is better than EmimDEP for dissolving cellulose. So, the σ-profile result can be used to describe the anions dissolution capacity when combined with the same cations. σ-profiles have also has been studied by Gonzalez-Miquel et al.[38] who used this method to successfully identify the better cations for ILs. Comparing the orders of the anions in the lnγ predictions of the Model 1 and Model 2 in Fig. 3 and Fig. 4 (blue colour region), it can be seen that the order of DEP^{-} and BEN^{-} is different for Model 1 and 2. According to Fig. 8, the σ-profile of Ben^{-} has a more complementary region around the peak of +0.006 e/Å^2 and +0.019 e/Å^2 than DEP^{-}. Therefore, Ben^{-} should be more to the left than DEP^{-} in the logarithmic activity coefficient figures. Model 2 predicts this better than Model 1. Overall, according to the prediction and experimental results, Model 2, the mid-monomer part of cellotriose model, is better than the glucose model (Model 1) and the mid-dimer cellotetraose model (Model 2).

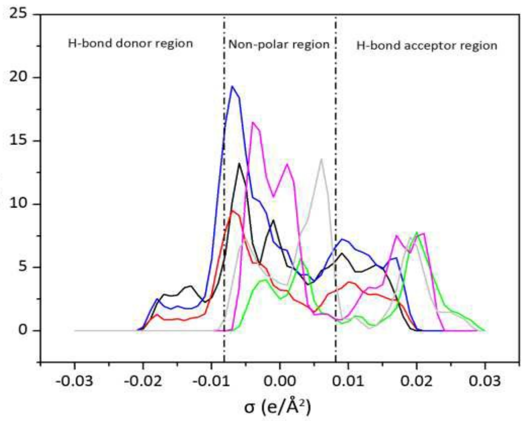

Fig. 8 σ-profiles of Model 1 (black line), Model 2 (red line), Model 3 (blue line) and anions Ac^{-} (green line), DEP^{-} (pink line) and BEN^{-} (grey line)

4. Experimental

4.1 Chemical reagents

Seven different ILs were synthesized and used for the experimental validation of the cellulose solubility results obtained from COSMO-RS. The initial synthetic materials included: 1-Methylimidazole (CP, Sinopharm Chemical Reagent Co., Lid.), Pyridine (⩾99.5%, Xilong Chemical Co., Ltd.), N-Ethylmorpholine (99%, aladdin), Allyl chloride (⩾97.0%, Sinopharm Chemical Reagent Co., Lid.), 2-Bromoethanol (97%, (Beijing) J&K Scientific LTD.), 2-Chloroethyl Methyl ether (98%, aladdin), Triethyl phosphate (CP, Sinopharm Chemical Reagent Co., Lid.), Ether absolute (99%, Tianjin jingdongtianzheng precision chemical reagent factory), Ethyl acetate (⩾99.5%, Xilong Chemical Co., Ltd.). Only 1-ethyl-3-methylimidazolium (99%) was purchased from Shanghai Cheng Jie Chemical Co. LTD. The other six ILs were synthesized in the lab. Microcrystalline cellulose was selected as the cellulose material (Column Chromatography, Sinopharm Chemical Reagent Co., Lid.) for the solubility analysis.

4.2 Nuclear magnetic resonance (NMR) and dissolution of MCC in ionic liquids

The structures of the seven ILs which were studied in this work can be seen in Scheme 1. The ILs were dried at 80 °C under vacuum for 48 hours after purification. The water content of each of the synthesized ILs was determined by Karl Fischer titration using a C20 Coulometric KF Titrator (Mettler Toledo Intl., Shanghai, China). Each of IL's water content was measured three times and the average value was used. The structures of these ILs were confirmed by ^{1}H NMR and ^{13}C NMR spectroscopy using a Bruker 600 spectrometer. The purities of the six synthesized ILs are HOEtmimBr (98.67 wt%), EtOMmimCl (99.31 wt%), EmimDEP (99.62 wt%), AmimCl (98.53 wt%), ApyCl (99.78 wt%), HOEtpyBr (98.33 wt%). The MCC was dried at 80 °C under vacuum for 48 h before use. MCC was added stepwise to a weighed amount of each of the seven ILs separately in a thermostatic oil bath at 90 °C. In the process of dissolution, an OLYMPUS BX 51 optical microscope was used to check the solubility of the MCC in these seven ILs. The limit of solubility was determined by gradually adding MCC until MCC could be observed under the optical microscope without dissolving after 12 hours.[35,44,45] The synthesis procedures and the properties of six synthesized ILs are shown in the supporting information.

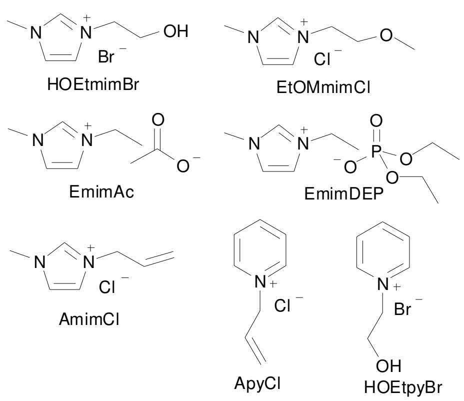

Scheme 1 The structures of the ILs synthesized and studied experimentally in this work

5. Conclusion

COSMO-RS was used to screen potential ILs for their ability to dissolve cellulose. Three cellulose representation models were tested in COSMO-RS. It was found that the mid-monomer part of cellotriose model is better to represent cellulose than the glucose model and mid-dimer part of cellotetraose model. The experimental solubilities of MCC in the ILs followed the trend prediction from the logarithmic activity coefficient values, except in the case of [EtOMmim]Cl The prediction of logarithmic activity coefficients of cellulose in ILs by COSMO-RS can therefore be considered an effective parameter to evaluate the dissolution power of the ILs. From the prediction results of the three cellulose models, it can be concluded that Ac$^-$, Dec$^-$, HCOO$^-$, Cl$^-$, BEN$^-$, DMPO$_4^-$, DEP$^-$, DBP$^-$ and Br$^-$ with various cations studied in this work are promising for cellulose dissolution. Cations with ethyl, allyl, 2-hydroxylethyl, 2-methoxyethyl and acryloyloxypropyl functional groups exhibited particularly good properties for cellulose dissolution. The excess enthalpy calculations indicated that the main forces in the cellulose dissolution in ILs are H-bonds, while the contribution of misfit forces and Van der Waals forces are secondary. The dissolution process is largely anion-dependent. Although there are divergences between the calculated and the experimental results, the main dissolution trend can be obtained from COSMO-RS predictions. The prediction of the capacity of ILs to dissolve cellulose may be further optimized by advancing the cellulose models even beyond the mid-monomer part of cellotriose and the mid-dimer part of cellotetraose cellulose models used here to obtain even more precise predictions that are in accord with experimental results. Further work may moreover encompass predictions considering the degree of cellulose crystallinity in different types of cellulose raw materials.

Acknowledgements

We sincerely thank Dr. Xiaochun Zhang, Dr. Feng Huo and Dr. Yongsheng Zhao for many helpful suggestions in the COSMO-RS calculation, and Wenjun Wang for helping with synthesis of ILs. This work was supported by the Department of Chemical and Biochemical Engineering, Technical University of Denmark and the National Natural Science Foundation of China (Grant No. 91434203 and 21576262), International S&T Cooperation Program of China (2014DFA61670) and CAS/SAFEA International Partnership Program for Creative Research Teams (20140491518).

References

1 C. Tsioptsias, A. Stefopoulos, I. Kokkinomalis, L. Papadopoulou and C. Panayiotou, *Green Chem.*, 2008, **10**, 965–971.

2 K. J. Edgar, C. M. Buchanan, J. S. Debenham, P. A. Rundquist, B. D. Seiler, M. C. Shelton and D. Tindall, *Prog. Polym. Sci.*, 2001, **26**, 1605–1688.

3 H. Wang, G. Gurau and R. D. Rogers, *Chem. Soc. Rev.*, 2012, **41**, 1519–1537.

4 D. M. Updegraff, *Anal. Biochem.*, 1969, **32**, 420–424.

5 H. Ohno, Y. Fukaya, *Chem. Lett.*, 2009, **38**, 2–7.

6 H. -P. Fink, P. Weigel, H. J. Purz and J. Ganster, *Prog. Polym. Sci.*, 2001, **26**, 1473–1524.

7 C. L. McCormick, T. R. Dawsey, *Macromolecules*, 1990, **23**, 3606–3610.

8 R. B. Hammer, A. F. Turbak, Abstracts of Papers of the American Chemical Society, 1977, **173**, 8.

9 S. Fischer, W. Voigt and K. Fischer, *Cellulose*, 1999, **6**, 213–219.

10 S. Fischer, H. Leipner, K. Thümmler, E. Brendler and J. Peters, *Cellulose*, 2003, **10**, 227–236.

11 K. Saalwächter, W. Burchard, P. Klüfers, G. Kettenbach, P. Mayer, D. Klemm and S. Dugarmaa, *Macromolecules*, 2000, **33**, 4094–4107.

12 Y. L. Zhao, X. M. Liu, J. J. Wang and S. J. Zhang, *J. Phys. Chem. B,* 2013, **117**, 9042–9049.

13 A. R. Xu, J. J. Wang and H. Y. Wang, *Green Chem.*, 2010, **12**, 268–275.

14 S. D. Zhu, Y. X. Wu, Q. M. Chen, Z. N. Yu, C. W. Wang, S. W. Jin, Y. G. Ding and G. Wu, *Green Chem*., 2006, **8**, 325–327.

15 R. P. Swatloski, S. K. Spear, J. D. Holbrey and R. D. Rogers, *J. Am. Chem. Soc.*, 2002, **124**, 4974–4975.

16 N. Sun, M. Rahman, Y. Qin, M. L. Maxim, H. Rodríguez and R. D. Rogers, Green Chem., 2009, **11**, 646–655.

17 M. Zavrel, D. Bross, M. Funke, J. Büchs and A. C. Spiess, *Bioresour. Technol.*, 2009, **100**, 2580–2587.

18 J. Palomar, J. S. Torrecilla, V. Ferro and F. Rodríguez, Eng. Chem. Res., 2009, **48**, 2257–2265.

19 M. Kosmulski, J. Gustafsson and J. B. Rosenholm, *Thermochim. Acta*, 2004, **412**, 47–53.

20 P. Mäki-Arvel, I. Anugwom, P. Virtanen, R. Sjöholm and J. P. Mikkola, *Ind. Crop. Prod.*, 2010, **32**, 175–201.

21 Y. Li, X. M. Liu, S. J. Zhang, Y. Y. Yao, X. Q. Yao, J. L. Xu and X. M. Lu, *Phys. Chem. Chem. Phys*., 2015, **17**, 17894–17905.

22 A. Casas, J. Palomar, M. V. Alonso, M. Oliet, S. Omar and F. Rodriguez. *Ind. Crop. Prod.*, 2012, **37**, 155–163.

23 I. Kilpeläinen, H. B. Xie, A. King, M. Granstrom, S. Heikkinen and D. S. Argyropoulos, *J. Agric. Food Chem.*, 2007, **55**, 9142–9148.

24 T. Erdmenger, C. Haensch, R. Hoogenboom and U. S. Schubert, *Macromol. Biosci.*, 2007, **7**, 440–445.

25 Y. L. Zhao, X. M. Liu, J. J. Wang and S. J. Zhang, *ChemPhysChem*., 2012, **13**, 3126–3133.

26 L. Feng, Z. L. Chen, *J. Mol. Liq.*, 2008, **142**, 1–5.

27 H. M. Luo, C. R. Zhou and Y. Q. Li, Polym. *Mater. Sci. Eng.*, 2005, **21**, 233–235.

28 H. Zhao, G. A. Baker, Z. Y. Song, O. Olubajo, T. Crittle and D. Peters, *Green Chem*., 2008, **10**, 696–705.

29 Z. Guo, B.-M. Lue, K. Thomsen, A. S. Meyer and X. Xu, *Green Chem*., 2007, **9**, 1362–1373.

30 A. Klamt, Advanced *Review*, 2011, **1**, 699-709.

31 M. Diedenhofen, A. Klamt, *Fluid Phase Equilib.*, 2010, **294**, 31–38.

32 A. Navas, J. Ortega, R. Vreekamp and E. Marrero, *Ind. Eng. Chem. Res.*, 2009, **48**, 2678–2690.

33 J. Palomar, M. Gonzalez-Miquel, A. Polo and F. Rodriguez, *Ind. Eng. Chem. Res.*, 2011, **50**, 3452–3463.

34 M. Gonzalez-Miquel, J. Palomar, S. Omar and F. Rodriguez, *Ind. Eng. Chem. Res.*, 2011, **50**, 5739–5748.

35 A. Casas, S. Omar, J. Palomar, M. Oliet, M. V. Alonsoa and F. Rodrigueza, *RSC Adv.*, 2013, **3**, 3453–3460.

36 C. Loschen, A. Klamt, *Ind. Eng.* Chem. *Res.*, 2014, **53**, 11478–11487.

37 J. Kahlen, K. Masuch and K. Leonhard, Green *Chem.*, 2010, **12**, 2172–2181.

38 M. Gonzalez-Miquel, M. Massel, A. DeSilva, J. Palomar, F. Rodriguez and J. F. Brennecke, *J. Phys. Chem. B*, 2014, **118**, 11512−11522.

39 D. G. Raut, O. Sundman, W. Q. Su, P. Virtanen, Y. Sugano, K. Kordas and J. Mikkola, *Carbohyd. Polym.*, 2015, 130, 18-25.

40 M. Zavrel, D. Bross, M. Funke, J. Büchs and A. C. Spiess, *Bioresource Technol.*, 2009, 100, 2580-2587.

41 A. M. Bochek, *Russ. J. Appl. Chem*., 2003, **76**, 1711−1719.

42 J. Vitz, T. Erdmenger, C. Haensch and U. S. Schubert, *Green Chem.*, 2009, 11, 417-424.

43 F. Huo, Z. P. Liu and W. C. Wang, *J. Phys. Chem. B*, 2013, 117, 11780-11792.

44 L. Liu, M. T. Ju, W. Z. Li, Q. D. Hou, *Carbohyd. Polym.*, 2013, 98, 412–420.

45 S. Agarwal, A. M. Hossain, Y. Choi, M. Cheong, H. G. Jang and J. S. Lee, *Bull. Korean Chem. Soc.*, 2013, 3771–3775.

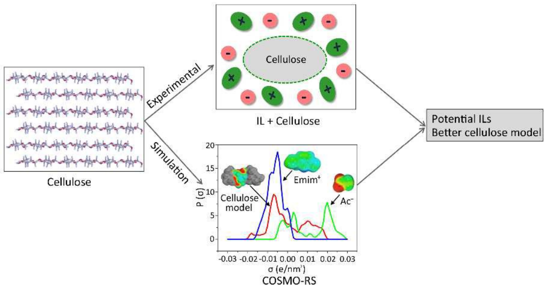
Cellulose
Experimental
Simulation
Cellulose
IL + Cellulose
+
-
Potential ILs
Better cellulose model
20
15
10
5
0
P (σ)
Cellulose model
Emim+
Ac−
-0.03 -0.02 -0.01 0.00 0.01 0.02 0.03
σ (e/nm²)
COSMO-RS